Original Article

Folia Primatol 2013;84:180–200
DOI: 10.1159/000351562

Received: December 10, 2012
Accepted after revision: April 19, 2013
Published online: July 18, 2013

Exploring Diagonal Gait Using a Forward Dynamic Three-Dimensional Chimpanzee Simulation

W.I. Sellers[a] L. Margetts[a] K.T. Bates[b] A.T. Chamberlain[a]

[a]University of Manchester, Manchester, and [b]University of Liverpool, Liverpool, UK

Key Words
Chimpanzee musculoskeletal simulation · Gait selection · Quadrupedalism

Abstract

Primates are unusual among terrestrial quadrupedal mammals in that at walking speeds they prefer diagonal rather than lateral gaits. A number of reasons have been proposed for this preference in relation to the arboreal ancestry of modern primates: stability, energetic cost, neural control, skeletal loading, and limb interference avoiding. However, this is a difficult question to explore experimentally since most primates only occasionally use anything other than diagonal gaits. An alternative approach is to produce biologically realistic computer simulations of primate gait that enable the constraints of biomechanical loading and the energetics of different modes of locomotion to be explored. In this paper we describe such a model for the chimpanzee *Pan troglodytes*. The simulation is able to produce spontaneous quadrupedal locomotion, and the footfall sequences generated are split between lateral and diagonal footfall sequences with no obvious energetic benefit associated with either option. However, out of 10 successful simulation runs, 5 were lateral sequence/lateral couplet gaits indicating a preference for a specific lateral footfall sequence with a relatively tightly constrained phase difference between the fore- and hindlimbs. This suggests that the choice of diagonal walking gaits in chimpanzees is not a simple mechanical phenomenon and that diagonal walking gaits in primates are selected for by multiple factors.

Introduction

In recent years, for those studying human biomechanics, the use of high biofidelity musculoskeletal models has become a standard technique with commercial (LifeMOD, SIMM, AnyBody, MADYMO, ADAMS) and freely available (Open-

KARGER

E-Mail karger@karger.com
www.karger.com/fpr

0015–5713/13/0845–0180$38.00/0

W.I. Sellers
Faculty of Life Sciences
University of Manchester, Michael Smith Building
Oxford Road, Manchester M13 9PT (UK)
E-Mail William.Sellers@manchester.ac.uk

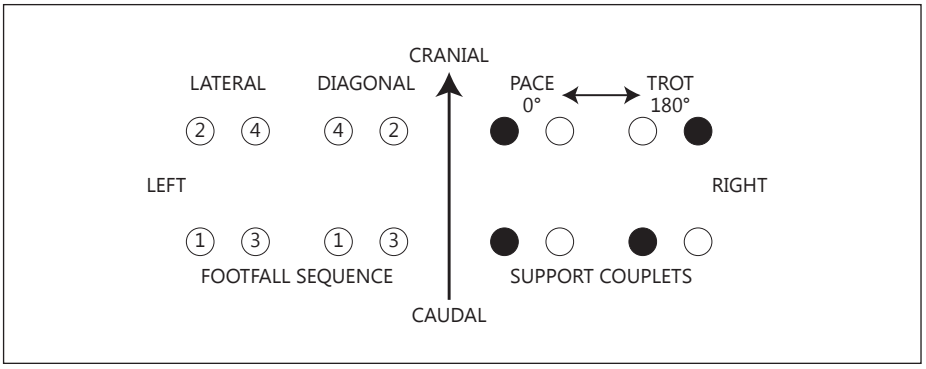

Fig. 1. Diagram illustrating the footfall sequences and support couplets associated with lateral and diagonal gaits.

SIMM, GaitSym) offerings available. The specific capabilities of these simulation packages vary quite widely but they all have access to detailed underlying musculoskeletal models that can either match recorded motion capture and external force data or generate locomotor movements de novo to optimise some global criteria such as the energetic cost of transport. More generally among primates there are fewer examples. There is a hindlimb-only model of *Australopithecus afarensis* [Nagano et al., 2005] which can generate hindlimb mechanics to move between specified postures at the start and end of an individual step. There is also a full quadrupedal Japanese macaque model [Ogihara et al., 2009] that has been used to match motion capture data [Ogihara et al., 2010]. In practice the major work package involved is in constructing the musculoskeletal model. Once created, porting a model to a different underlying simulation architecture is usually relatively straightforward. The basic morphological data required are identical although the formulation of specific elements will vary depending on what is available in each software package. This includes aspects such as the force generation model used for muscles and the contact models used to simulate the reaction forces generated by ground contact. Once created these models can be adapted for a range of locomotor studies and it is therefore important that they are made publicly available if at all possible, particularly since this allows other researchers to independently replicate any findings.

Animals are defined by the way they move and locomotion is clearly of fundamental biological importance. Quadrupedal animals regularly use a range of different locomotor styles (walks, trots, paces, canters and gallops) and these are generally characteristic of a particular species. Western interest in animal gait can be traced back to the origins of dressage in the 16th century, and whilst we have been able accurately to catalogue and quantify the various gaits used since the 1960s [Hildebrand, 1965, 1967, 1968], our understanding of what factors determine the optimality of particular gaits remains poor. Primates are a particularly interesting case. They have a very unusual diagonal sequence of footfalls (left hind, followed by right fore, then right hind, then left fore, as illustrated in fig. 1) at walking speeds, and generally they transition from walking directly to galloping without an intermediate trotting phase

Table 1. The relationship between descriptive footfall pattern names and the percentage of the gait cycle that the footfall of the forefoot follows the footfall of the hindfoot on the same side [Hildebrand, 1965]

Phase lag minimum, %	Phase lag maximum, %	Sequence name	Couplet name
0	5	Pace	
5	20	Lateral sequence	Lateral couplets
20	30		Singlefoot
30	45		Diagonal couplets
45	55	Trot	
55	70	Diagonal sequence	Diagonal couplets
70	80		Singlefoot
80	95		Lateral couplets
95	100	Pace	

[Higurashi et al., 2009]. Additionally this diagonal gait pattern is preserved in other locomotor modes such as climbing [Hirasaki et al., 2000] and even in human bipedal locomotion where arm swinging is diagonally out of phase with footfalls [Wang et al., 2003] and where diagonal gaits predominate in the short postnatal quadrupedal crawling stage [Patrick et al., 2009]. Finally, primates have other quadrupedal locomotor peculiarities such as longer than predicted stride lengths [Alexander and Maloiy, 1984], the use of highly flexed limbs during locomotion [Schmitt, 2003], and the so-called hindlimb drive with the hindlimb tending to experience greater propulsive, braking and vertical forces than the forelimb [Kimura et al., 1979; Demes et al., 1994; Kimura, 2000]. Suggested reasons for primate gait choices include energetics [Griffin et al., 2004], stability [Cartmill et al., 2002], and neural control [Vilensky, 1987], but other factors such as skeletal loading [Raynor et al., 2002] and limb interference avoiding [Hildebrand, 1980] have also been suggested as drivers for quadrupedal gait choice and may be equally important.

A number of approaches have been applied to the study of footfall patterns in primates. Initially the main interest was in cataloguing the differences between different primate species moving quadrupedally, including human children, pioneered by Hildebrand [1967] using much more rigorous cinematographic techniques compared to unassisted observation that had been favoured previously [Magna De La Croix, 1929]. Hildebrand found a great range of gaits used by primates and he classified them based on the percentage of the gait cycle that the footfall of the forefoot follows the footfall of the hindfoot on the same side. Descriptively this characterises and identifies the footfall sequences: diagonal sequences with long ipsilateral phase lags (left hind, right fore, right hind, left fore) or lateral sequences with short ipsilateral phase lags (left hind, left fore, right hind, right fore), and footfall couplets (which pair of feet spends most of the time on the ground together): lateral (both left limbs paired, both right limbs paired) or diagonal couplets (left hind and right fore paired, right hind and left fore paired). Table 1 shows how these descriptive names correspond to the phase lag [Hildebrand, 1965]. Figure 1 illustrates how footfalls are counted to identify lateral and diagonal gaits, and shows how there is a continuum of footfall

overlap from pacing where there is no overlap but both feet on one side of the body hit the ground together, and trotting where there is again no overlap but in this case feet on opposite sides of the body hit the ground together. Diagonal couplet gaits are those whose phase relationship is closer to trotting, and lateral couplets are those whose phase relationship is closer to pacing. The precise values chosen for these names are not absolute and reflect the fact that Hildebrand found variation of at least 10 percentage points in measured phase lags between different horses performing particular gaits [Hildebrand, 1965]. This is also a considerable simplification of all possible symmetrical footfall patterns. Using this classification system, the majority of quadrupedal animals demonstrate lateral sequence walking gaits. Primates generally use diagonal sequence/diagonal couplet gaits. The other diagonal sequence options are not generally seen in any quadruped at natural walking speeds. The use of other phase relationships among primates, particularly with phases from the 20- to 55-degree range, is occasionally seen and is sometimes the preferred gait, particularly in infants and juveniles [Hildebrand, 1967].

Whilst there has been considerable empirical work on quantifying primate gait choice [for extensive reviews, see Vilensky and Larson, 1989; Schmitt, 2003], there have been far fewer theoretical analyses. One of the most influential is the suggestion that primates use diagonal gaits to maximise stability [Cartmill et al., 2002]. Stability may be a relatively important factor in primates, given their use of arboreal substrates with irregularly spaced, angled and compliant supports. In addition, primates have relatively longer limbs and longer step lengths compared to mammals of similar body size, which may tend to compromise stability during primate quadrupedal locomotion. The stability maximisation model makes specific predictions about the need to minimise periods of bipedality whether using diagonal or lateral sequences. It also makes explicit the fact that symmetrical gaits can be entirely defined by 3 parameters: the phase difference between the fore- and hindlimbs, and the duty factors of the fore- and hindlimbs (duty factor is the proportion of the gait cycle for which a limb maintains contact with the substrate). This was recognised by Hildebrand [1965] but not dealt with in his analysis where the duty factor was considered the same for both fore- and hindlimbs.

In addition to stability, a number of other reasons for quadruped gait choices have been suggested. These include considerations of energetics, as different gaits are more or less effective at recovering energy from accelerated body segments [Griffin et al., 2004], and neural control, as stepping movements in primates appear to be controlled by supraspinal neural circuits, rather than by spinal central pattern generators as in non-primate mammals [Vilensky, 1987]. However, other factors such as skeletal loading, the need to maintain peak mechanical stresses below critical thresholds to avoid damage to the musculoskeletal system [Raynor et al., 2002], and avoidance of limb interference, which may arise in relatively long-limbed animals [Hildebrand, 1980], have been suggested to influence gait choice in other quadrupeds and these may also apply to primates. These hypotheses are not mutually exclusive and the importance of each may depend on speed and substrate. We also do not exclude the intriguing possibility that primate gait choice may also be a dynamic phenomenon that allows efficient gait change. Investigating these hypotheses is non-trivial. Most work with primates is necessarily purely observational with very limited opportunities for training except in exceptional cases (e.g. bipedally trained macaques [Nakatsukasa et al., 2004]) so that obvious approaches such as training an animal to adopt a range of

different quadrupedal gaits, as is done for dressage horses, are not possible. Sophisticated work has been done looking at changes in gait with age [Shapiro and Raichlen, 2005] and substrate [Higurashi et al., 2009] but these are primarily observational rather than interventional approaches and so the findings cannot be interpreted unambiguously. An alternative, complementary approach that can overcome some of these difficulties is the use of computer simulations since these can be used to address a range of 'what if' questions in primate locomotor biology since they allow investigative paradigms such as 'virtual ablation' [Sellers et al., 2010] that have no direct experimental equivalence.

The aims of the current study were to construct a virtual musculoskeletal model of a chimpanzee, to explore its range of locomotor performance (preferred gaits, velocity or travel and energetic costs) using repeated trials in the GaitSym computer simulation package (http://www.animalsimulation.org), to test whether the model converges on a stable gait solution, and to determine whether the model can allow us to discern amongst the major hypotheses for the predominant use of diagonal walking gaits among primates.

Methods

A 3-dimensional musculoskeletal model contains a number of elements: a skeleton that defines the rigid links within the model; a series of joints that connect and permit specified movements between the individual links; muscles that are rigged onto the skeleton and actuate joint movements; contact points that allow the model to interact with the substrate, and a series of drivers that activate the muscles. The starting point for the model was a full-body CT scan of an adult male chimpanzee that died of natural causes (with no obvious musculoskeletal defects) at the Welsh Mountain Zoo in the UK. As is common with zoo animals, this individual was eviscerated during a veterinary post mortem examination but otherwise was complete. The CT scan was performed in several sections with variable resolution and slice spacing (skull 1-mm slices; thorax and forelimb 3 mm; pelvis and hindlimb 2 mm). The skin outline and the bone outlines were extracted using isosurfacing at suitable density levels using Osirix v3.5 (http://www.osirix-viewer.com). However, these isosurfaces are not particularly suitable in their raw state and so the meshes generated were cleaned up using Geomagic Studio 12 (http://www.geomagic.com). Using Geomagic, the isosurface meshes were edited to remove obvious artefacts, the polygon count was reduced, and the surfaces were smoothed. Geomagic also allowed the isosurfaces from multiple slices to be accurately merged to form a complete body reconstruction. Subsequently the segments were isolated to produce sets of skin outlines and sets of bones. Only one side of the appendicular skeleton was cleaned up in this way with the opposite side being produced by mirroring. The choice of side varied depending on the quality of the extracted isosurface. The isolated segments were then imported into 3DS Max (http://www.autodesk.com) where individual segments were posed to produce a standard anatomical position. In particular the torso needed considerable straightening in the lumbar region. However, where possible, reposing was performed by rotating at joint centres in order to maintain an anatomical joint spacing. Because of the evisceration it was not possible to complete the reconstruction of the trunk with very high accuracy, and in particular the skin outline for this region was not usable.

The posed bony skeleton defines the geometry of the model. The joint centres can be measured directly off the scanned skeleton, as can the origin, insertion and paths of individual muscles. This was performed within GaitSym. The skin outlines, after segmentation, can be converted into closed triangular meshes. These were then used to calculate the segment mass properties, again within GaitSym, using chimpanzee segment densities where available [Crompton et al., 1996] and human densities otherwise [Winter, 1990]. There remains the question of what to do about the trunk because of the damage done by the autopsy. Because the skeleton outline was

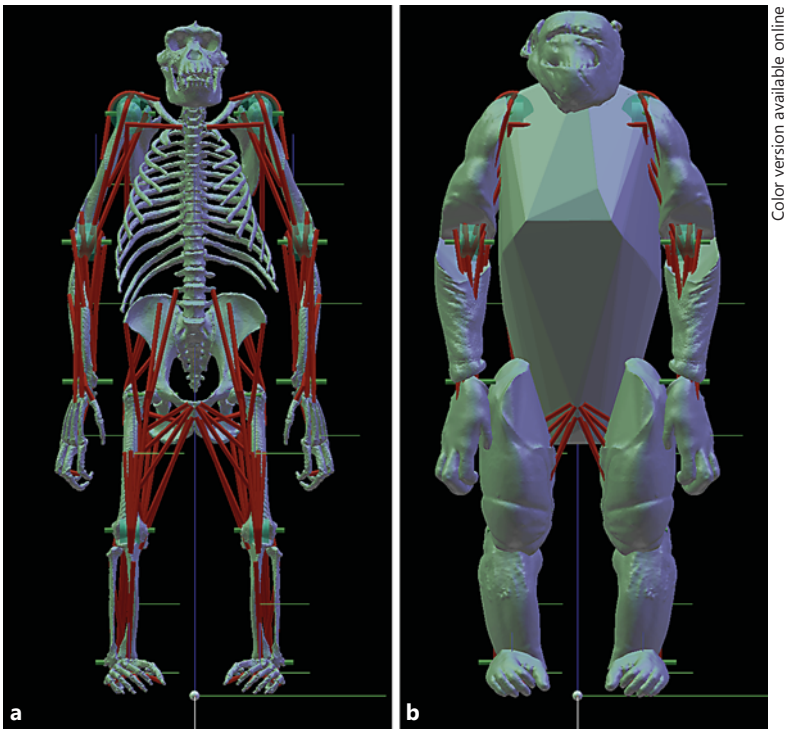

Fig. 2. Chimpanzee model standing in the anatomical position illustrating how the bone model (**a**) relates to the skin model (**b**) and showing how the convex hull has been formed over the torso skeleton.

available it was felt that wrapping this outline should produce a better estimate of mass properties than previous suggestions that rely on a much smaller subset of measurements [Crompton et al., 1996]. Wrapping was therefore performed using the *qhull* function in Matlab (http://www.mathworks.com) to produce a minimum convex polygon enclosing the shoulder and pelvic girdles, the spine and ribcage. The results of this procedure can be clearly seen in figure 2 and a summary of the calculated mass properties is shown in table 2. Volumetric approaches are a well-known alternative to pendulum-based methods [Bates et al., 2009] and have the advantage of producing a complete set of both products and moments of inertia which are otherwise rarely reported. The volumetric analysis gave an estimated body mass for the subject of 66.5 kg. Note this estimate is within the normal range for captive chimps [Videan et al., 2007], but very high compared to the median mass of wild male animals [Pusey et al., 2005].

The joints are represented as abstract engineering joints: hinge joints, ball joints and universal joints. These work well for the hip and elbow, and are reasonable approximations for the ankle and wrist joints. However, they do not work particularly well for knee and shoulder joints at the extremes of joint movement and this is an area that needs further work. For kinematic matching, explicit joint limits are not required since the range of movement is defined by the applied kinematics [Ogihara et al., 2010]. However, when used for de novo gait generation joint limits are required to specify the range of movement available. These work well for hinge joints but there are mathematical difficulties applying joint limits particularly to ball joints when the allowable range of movement is large. In addition whilst we have some idea of joint limits in in-

Table 2. The mass properties calculated for the model

Segment name	Mass kg	I11 kg·m^2	I22 kg·m^2	I33 kg·m^2	I12 kg·m^3	I13 kg·m^3	I23 kg·m^3	X m	Y m	Z m
Left arm	2.935	0.0175	0.0194	0.0072	0.0000	–0.0026	0.0033	0.053	0.197	1.022
Left foot	0.910	0.0010	0.0026	0.0029	0.0003	0.0000	0.0000	0.090	0.131	0.045
Left forearm	2.138	0.0110	0.0127	0.0042	–0.0001	0.0030	–0.0007	0.077	0.233	0.784
Left hand	0.901	0.0034	0.0034	0.0009	0.0002	–0.0001	0.0005	0.116	0.229	0.520
Left shank	2.483	0.0163	0.0162	0.0038	0.0003	–0.0015	–0.0013	0.045	0.130	0.184
Left thigh	6.668	0.0602	0.0688	0.0240	–0.0020	0.0053	–0.0028	0.054	0.121	0.484
Right arm	2.935	0.0175	0.0194	0.0072	0.0000	–0.0026	–0.0033	0.053	–0.197	1.022
Right foot	0.910	0.0010	0.0026	0.0029	–0.0003	0.0000	0.0000	0.090	–0.131	0.045
Right forearm	2.138	0.0110	0.0127	0.0042	0.0001	0.0030	0.0007	0.077	–0.233	0.784
Right hand	0.901	0.0034	0.0034	0.0009	–0.0002	–0.0001	–0.0005	0.116	–0.229	0.520
Right shank	2.483	0.0163	0.0162	0.0038	–0.0003	–0.0015	0.0013	0.045	–0.130	0.184
Right thigh	6.668	0.0602	0.0688	0.0240	0.0020	0.0053	0.0028	0.054	–0.121	0.484
Trunk	34.392	1.5471	1.4787	0.3022	0.0038	–0.1422	0.0034	0.060	0.000	0.949

The I values are the elements of the 3-dimensional inertial tensor with the first digit representing the row and the second digit representing the column. The XYZ values are the positions of the segment centres of mass in global model coordinates in the anatomical position. The off diagonal terms are simply minus the products of inertia, and I12 and I23 have opposite signs on the different sides of the body.

dividual axes, these limits are not independent and there is no information on the interaction of joint limits with joint pose beyond qualitative observations which are particularly complex at the shoulder. For this reason we are currently limited to hinge joints for the de novo gait generation model where the joint ranges have been limited to those reported for bipedal and quadrupedal gait [Watson et al., 2009]: effectively physiological limits for this particular set of movements rather than anatomical limits. These joint limits would need to be altered if the model was to be used for other simulation purposes. Additional movement constraints are provided by contact points positioned on the foot and the hand segments. These are represented as 5-mm diameter incompressible spheres and they generate the necessary forces to prevent interpenetration when they touch the ground plane in the model. The locations of the joint and contact centres are given in table 3.

Muscle paths are defined using anatomical knowledge of the origins, insertions and relations of the individual muscles. In general, a muscle can be considered as a tension-generating machine that acts between two points attached to the skeleton. To accommodate muscles that do not follow a straight line, we can define wrapping operators that allow the muscle to bend around other structures and apply appropriate forces when they do so. GaitSym has two wrapping operators. Via points have a function very similar to anatomical retinacula and provide pulley points that change the line, of action of the muscle. Cylinder wrapping is also implemented that allows the muscle path to wrap around a virtual cylinder attached to the skeleton to imitate the action of a muscle wrapping around a bone. These operators provide a reasonable level of biorealism at minimal computational cost but there are particular issues that they cannot cope with. Muscles such as the M. dorsoepitrochlearis brachii originate on the tendon of the M. latissimus dorsi and the mechanics of this arrangement currently cannot be well represented. Instead an origin close to the insertion of the M. latissimus dorsi on the humerus was chosen. Via points need to be selected with a great deal of care because they move with the skeleton. This means that it is very easy to end up with a situation where at one extreme of joint movement there is an unrealistic reduction in moment arm and at the other extreme via points overlap so

Table 3. The joint and contact centres used in the model

Joint or contact name	X m	Y m	Z m
Right hip joint centre	0.012	–0.084	0.601
Right knee joint centre	0.046	–0.130	0.331
Right ankle joint centre	0.016	–0.147	0.066
Right shoulder joint centre	0.070	–0.128	1.163
Right elbow joint centre	0.078	–0.215	0.906
Right wrist joint centre	0.113	–0.213	0.628
Right posterior medial foot contact	0.007	–0.145	0.010
Right posterior lateral foot contact	0.007	–0.154	0.009
Right metatarsal medial contact	0.113	–0.080	0.050
Right metatarsal lateral contact	0.125	–0.169	0.029
Right proximal medial knuckle contact	0.143	–0.226	0.445
Right proximal lateral knuckle contact	0.109	–0.269	0.444
Right distal medial knuckle contact	0.118	–0.212	0.434
Right distal lateral knuckle contact	0.088	–0.241	0.431

The XYZ values are given in global model coordinates in the anatomical position.

that the path of action of the muscle becomes a very unrealistic zigzag. Cylinder wrapping can avoid these problems but cylinders are only suitable in very specific situations and only one cylinder can be used on an individual muscle. General solutions to wrapping muscles can be implemented using sliding contacts but these are computationally extremely expensive and so rarely used. Muscle geometry was taken from the literature and scaled geometrically to match the body size of the subject animal. Linear measures were scaled by $mass^{1/3}$, areas by $mass^{2/3}$. There are several studies comparing individual muscles, or where a single limb has been considered [Payne et al., 2006; Oishi et al., 2009; Myatt et al., 2011]. However, for a quadrupedal model we need a complete muscle set. There is only a single example of an animal where both the forelimb and hindlimb muscles were measured together [Thorpe et al., 1999] and this individual was similarly eviscerated before dissection which meant that several key muscles were missing. M. iliacus and M. psoas major muscle geometries were obtained by scaling their sizes relative to M. rectus femoris from a *Pan paniscus* hindlimb dissection [Payne et al., 2006]. This is not ideal but, as Payne et al. show, *P. paniscus* has the most similar hindlimb muscle geometry patterns to *P. troglodytes*. M. pectoralis major muscle mass was scaled from M. latissimus dorsi mass using a published mass ratio [Ziegler, 1964]; its fibre length was scaled from M. latissimus dorsi fibre length using a different published ratio [Carlson, 2006], and its physiological cross-section area was then calculated from its volume using a density of 1,060 $kg \cdot m^{-3}$ [Méndez and Keys, 1960]. The complete set of values is given in table 4a and b for muscle geometric properties and for origins and insertions.

The musculoskeletal model was implemented in the GaitSym simulation package. To investigate the mechanics of quadrupedal walking it is necessary to generate activation patterns for the muscles that produce the required range of footfall patterns. Previous experience has shown that walking gaits for bipeds can be obtained by optimising for minimal energetic cost of locomotion using a genetic algorithm search procedure [Sellers et al., 2003]. To our knowledge such a procedure has not been published for biorealistic quadrupedal simulation but has proved successful for generating quadrupedal running gaits when optimised for maximum speeds [Sellers et al., 2009] and pilot experimentation with simplified horse and orangutan models has successfully generated a range of gaits. We thus used our standard gait morphing methodology [Sellers et al.,

Table 4. Muscle properties for the limb muscles
a Hindlimbs

Muscle names	Muscle mass kg	Fascicle length m	PCSA m^2	OX m	OY m	OZ m	IX m	IY m	IZ m
M. adductor brevis	0.092	0.185	0.00047	0.061	–0.010	0.573	0.036	–0.114	0.477
M. adductor longus	0.227	0.195	0.00110	0.068	–0.005	0.578	0.054	–0.119	0.402
M. adductor magnus	0.209	0.210	0.00094	0.058	–0.004	0.557	0.048	–0.098	0.343
M. biceps femoris (long head)	0.085	0.157	0.00051	–0.017	–0.088	0.532	0.021	–0.159	0.298
M. biceps femoris (short head)	0.049	0.100	0.00046	0.026	–0.132	0.423	0.021	–0.159	0.298
M. flexor digitorum longus	0.041	0.053	0.00072	0.034	–0.124	0.221	0.173	–0.105	0.018
M. flexor hallucis longus	0.081	0.064	0.00120	0.021	–0.163	0.221	0.145	–0.066	0.028
M. gastrocnemius lateralis	0.067	0.080	0.00079	0.036	–0.138	0.360	–0.017	–0.155	0.034
M. gastrocnemius medialis	0.090	0.080	0.00106	0.039	–0.117	0.358	–0.017	–0.155	0.034
M. gluteus maximus	0.300	0.101	0.00279	–0.022	–0.039	0.743	0.004	–0.139	0.540
M. gluteus medius	0.269	0.088	0.00288	–0.013	–0.072	0.774	–0.004	–0.137	0.613
M. gluteus minimus	0.069	0.065	0.00100	–0.005	–0.106	0.729	–0.004	–0.137	0.613
M. gracilis	0.120	0.225	0.00050	0.049	–0.012	0.552	0.044	–0.109	0.293
M. iliacus	0.163	0.090	0.00171	–0.005	–0.069	0.784	–0.003	–0.102	0.558
M. obturatorius externus	0.050	0.068	0.00069	0.029	–0.022	0.546	–0.017	–0.108	0.569
M. pectineus	0.036	0.105	0.00033	0.071	–0.012	0.583	0.006	–0.115	0.520
M. peroneus longus	0.050	0.050	0.00095	0.025	–0.165	0.278	0.085	–0.120	0.049
M. psoas major	0.100	0.220	0.00043	0.008	–0.036	0.811	–0.003	–0.102	0.558
M. rectus femoris	0.093	0.078	0.00113	0.017	–0.083	0.670	0.066	–0.128	0.285
M. sartorius	0.058	0.300	0.00018	0.017	–0.137	0.745	0.025	–0.099	0.295
M. semimembranosus	0.067	0.158	0.00040	–0.012	–0.074	0.517	0.026	–0.112	0.287
M. semitendinosus	0.100	0.260	0.00036	–0.012	–0.088	0.524	0.026	–0.112	0.287
M. soleus	0.128	0.055	0.00220	0.028	–0.135	0.291	–0.017	–0.155	0.034
M. tibialis anterior	0.050	0.088	0.00053	0.066	–0.122	0.268	0.053	–0.133	0.070
M. tibialis posterior	0.065	0.025	0.00246	0.032	–0.126	0.254	0.049	–0.133	0.048
M. vastus intermedius	0.133	0.090	0.00139	0.041	–0.127	0.490	0.066	–0.128	0.285
M. vastus lateralis	0.220	0.100	0.00208	0.037	–0.139	0.486	0.066	–0.128	0.285
M. vastus medialis	0.102	0.096	0.00100	0.038	–0.117	0.486	0.066	–0.128	0.285

2004]. The animal model is initially positioned in a stationary quadrupedal stance. The genetic algorithm then searches for a cyclic activation pattern that maximises the forward distance travelled for 10,000 J of energy. This value is calculated using a mathematical model of the metabolic cost of muscle contraction [Minetti and Alexander, 1997]. Finding an accelerating pattern like this is very difficult and this does not produce very high-quality gait so for subsequent repeats the starting conditions are taken from a mid-simulation cycle of a previous run. Using this approach iteratively the algorithm eventually converges on a constant velocity solution. Genetic algorithm search is not exhaustive so individual runs can produce very different results. This means that from the same starting conditions and after the gait morphing process has been repeated a number of times, we can end up with a range of gaits that all represent reasonable solutions to the global optimisation target of travelling forward for minimal energy. To allow some sort of objective comparison we repeated the standing start process until we had 10 examples where the simulation managed to travel more than approximately 4 m and hence had achieved a regular gait cycle. This occurred in about half the cases. We then used equivalent computational effort to try and improve on these 10 sets of starting conditions using the gait-morphing procedure. The equivalent computational effort was 9 h running on 6,144 cores on the Hector Phase 2b Cray XT6 system for each starting condition (a total of well over 500,000 core hours of computing time).

Table 4 (continued)
b Forelimbs

Muscle names	Muscle mass kg	Fascicle length m	PCSA m^2	OX m	OY m	OZ m	IX m	IY m	IZ m
M. abductor pollicis longus	0.032	0.040	0.00076	0.063	–0.250	0.801	0.136	–0.202	0.590
M. biceps brachii (brevis)	0.108	0.150	0.00068	0.079	–0.096	1.165	0.088	–0.222	0.858
M. biceps brachii (longus)	0.088	0.125	0.00067	0.062	–0.125	1.200	0.088	–0.222	0.858
M. brachialis	0.133	0.092	0.00136	0.094	–0.173	1.049	0.073	–0.219	0.868
M. brachioradialis	0.114	0.175	0.00061	0.082	–0.226	0.966	0.126	–0.199	0.648
M. coracobrachialis	0.038	0.056	0.00063	0.078	–0.095	1.160	0.078	–0.174	1.017
M. deltoideus	0.276	0.083	0.00314	0.049	–0.071	1.189	0.082	–0.184	1.071
M. dorsoepitrochlearis	0.043	0.095	0.00043	0.065	–0.147	1.111	0.037	–0.213	0.921
M. extensor carpi radialis brevis	0.038	0.090	0.00040	0.067	–0.232	0.910	0.134	–0.224	0.596
M. extensor carpi radialis longus	0.044	0.115	0.00036	0.082	–0.226	0.966	0.134	–0.224	0.596
M. extensor digitorum	0.048	0.060	0.00076	0.067	–0.232	0.910	0.124	–0.237	0.586
M. flexor carpi radialis	0.056	0.070	0.00075	0.084	–0.202	0.897	0.123	–0.216	0.584
M. flexor carpi ulnaris	0.065	0.052	0.00119	0.048	–0.177	0.912	0.084	–0.224	0.609
M. flexor digitorum profundus	0.176	0.154	0.00108	0.064	–0.222	0.845	0.086	–0.231	0.442
M. flexor digitorum superficialis	0.130	0.068	0.00180	0.070	–0.190	0.922	0.116	–0.242	0.487
M. infraspinatus	0.116	0.068	0.00161	–0.005	–0.117	1.011	0.089	–0.133	1.186
M. latissimus dorsi	0.373	0.240	0.00147	0.054	–0.135	0.929	0.090	–0.135	1.140
M. pectoralis major	0.266	0.196	0.00128	0.099	–0.025	1.136	0.093	–0.138	1.142
M. pronator teres	0.044	0.066	0.00064	0.057	–0.185	0.921	0.116	–0.209	0.772
M. supinator	0.039	0.035	0.00105	0.088	–0.244	0.931	0.122	–0.221	0.776
M. teres major	0.073	0.142	0.00048	–0.010	–0.116	1.002	0.078	–0.138	1.121
M. triceps brachii (long)	0.133	0.100	0.00126	0.053	–0.137	1.126	0.037	–0.213	0.921
M. triceps brachii (medial)	0.201	0.090	0.00211	0.065	–0.172	1.088	0.037	–0.213	0.921

PCSA = Physiological cross-sectional area; OX, OY, OZ are the origins of the muscles, and IX, IY, IZ are the insertions. These values are given in global model coordinates in the anatomical position.

The process of gait morphing was fully automated and an asynchronous implementation of the genetic algorithm was used to ensure that all cores were fully utilised during the optimisation (over 90% core utilisation was achieved). The resultant gait simulations were then evaluated using a custom Matlab script to identify the duty factors of the fore- and hindlimbs and phase relationship.

Results

All of the 10 gaits generated were stable over a distance of 8 m. However, their footfall pattern was highly varied, encompassing most of the Hildebrand classifications. Table 5 shows the phase relationships and the equivalent Hildebrand classifications [Hildebrand, 1965]. The algorithm generated 4 diagonal sequences and 6 lateral sequences. This would suggest no predominant preference for either sequence within the algorithm. Of the lateral sequences all but one were lateral couplet gaits,

Table 5. Phase relationships and duty factors of the simulated gaits

Run No.	Ipsilateral forelimb lag	Hindlimb duty factor	Forelimb duty factor	Sequence name	Couplet name
1	0.192	0.496	0.383	lateral sequence	lateral couplets
2	0.199	0.517	0.519	lateral sequence	lateral couplets
3	0.703	0.454	0.312	diagonal sequence	singlefoot
4	0.831	0.455	0.341	diagonal sequence	lateral couplets
5	0.196	0.386	0.468	lateral sequence	lateral couplets
6	0.163	0.499	0.478	lateral sequence	lateral couplets
7	0.394	0.521	0.501	lateral sequence	diagonal couplets
8	0.856	0.479	0.332	diagonal sequence	lateral couplets
9	0.627	0.504	0.470	diagonal sequence	diagonal couplets
10	0.163	0.499	0.527	lateral sequence	lateral couplets

The gait names refer to the Hildebrand classifications in table 1 [Hildebrand, 1965].

Table 6. The performance parameters of the individual simulated gaits

Run No.	Cycle time, s	Simulation time, s	Distance m	Velocity $m \cdot s^{-1}$	Cost of locomotion $J \cdot kg^{-1} \cdot m^{-1}$
1	0.954	7.587	8.395	1.106	8.962
2	0.885	5.475	8.030	1.467	9.369
3	0.688	6.072	8.729	1.437	8.619
4	0.694	5.186	9.694	1.869	7.761
5	0.836	6.193	7.949	1.284	9.464
6	0.687	7.128	9.675	1.357	7.776
7	0.989	10.241	9.820	0.959	7.661
8	0.647	5.497	8.882	1.616	8.470
9	0.790	5.931	9.309	1.570	8.081
10	0.850	8.150	9.154	1.123	8.218

which is the most common combination amongst quadrupeds. However, the diagonal sequences included both diagonal couplets (the prevalent primate condition), lateral couplets, and a singlefoot: these latter two are both very unusual gaits. Neither trotting nor pacing gaits were seen but the duty factors were generally rather low for walking gaits, suggesting these were approaching the maximum walking speed (although there were no completely aerial phases in any of the gaits). Figures 3 and 4 show examples of lateral and diagonal sequence gaits. The phase relationships observed are shown in figure 5. If there were no phase preference in the simulation, then the phase relationships would be uniformly spread over the range of 0–100% so that with 10 repeats, the expected value would be a frequency of 1 in each 10% subrange.

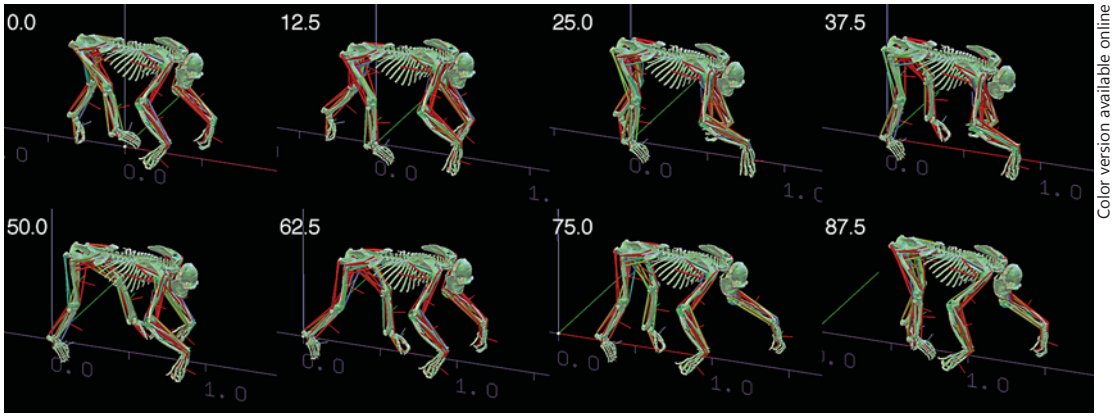

Fig. 3. Lateral sequence/lateral couplet animation sequence from GaitSym. This is run 10 and represents a complete gait cycle (duration 0.850 s).

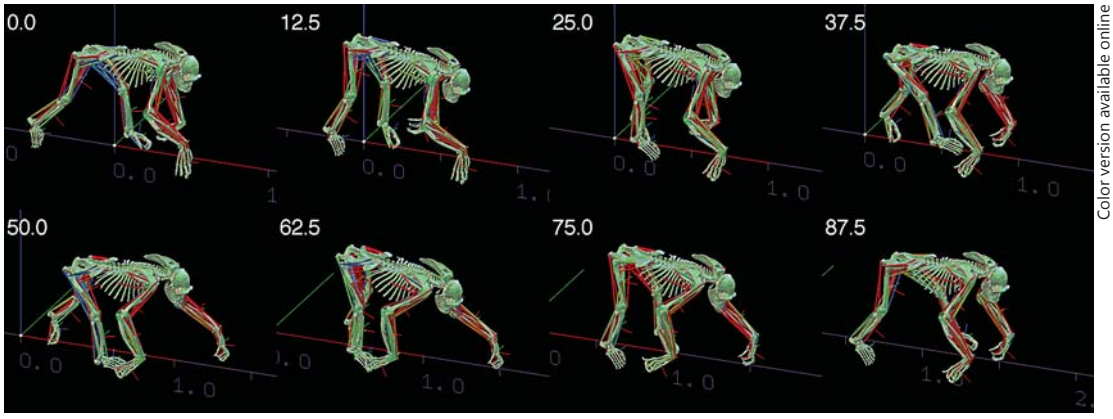

Fig. 4. Diagonal sequence/diagonal couplet animation sequence from GaitSym. This is run 9 and represents a complete gait cycle (duration 0.790 s).

This is clearly not the case with a frequency of 5 in the 10–20% range (lateral sequence, lateral couplet) and 2 in the 80–90% range (diagonal sequence, lateral couplet). The χ^2 goodness of fit value is 22, and using resampling to estimate the p value to avoid any problems with expected values being less than 5 gives a $p = 0.0057$ after 100,000 trials.

Table 6 shows the performance characteristics of the generated gaits. Whilst there is considerable variation in footfall pattern, there is relatively little variation in the energetic costs of the different gaits. To investigate whether there were any patterns to the variation, regression analysis was performed. Figure 6 shows the relationships between velocity and cycle time, cost of locomotion, hindlimb duty factor and forelimb duty factor. They all show rather predictable trends with falling cycle time,

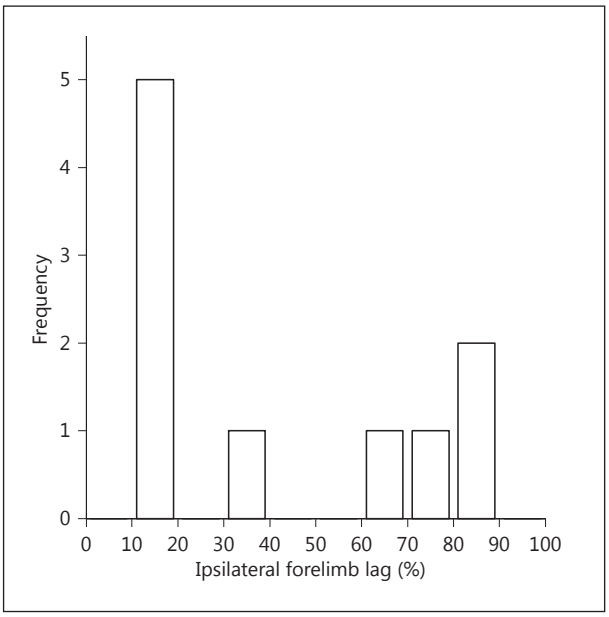

Fig. 5. Bar chart showing the frequency of individual phase relationships between the fore- and hindlimbs in the 10 simulations generated.

cost of locomotion, hindlimb duty factor and forelimb duty factor as the velocity increases. However, only the velocity and cycle time relationship is statistically significant: Pearson linear correlation coefficient = –0.759, p = 0.011. There are insufficient repeats to compare all the possible phase combinations but the 6:4 split does allow the comparison of diagonal versus lateral sequences and this is shown in figure 7. This figure shows the effect of lateral or diagonal footfall sequences on the mean cycle time, velocity, cost of locomotion, hindlimb duty factor and forelimb duty factor. Using independent t tests to compare the means, cycle time (d.f. = 8, t = 2.737, p = 0.026), velocity (d.f. = 8, t = –3.419, p = 0.009), and forelimb duty factor (d.f. = 8, t = 2.966, p = 0.018) are significantly different between lateral and diagonal sequences.

Discussion

We can suggest 5 possible reasons for primate footfall sequences: stability [Cartmill et al., 2002], energetics [Griffin et al., 2004], neural control [Vilensky, 1987], skeletal loading [Raynor et al., 2002], and limb interference avoidance [Hildebrand, 1980]. The chimpanzee simulation is able to generate spontaneous gait covering a range of phase relationships demonstrating a great deal of locomotor flexibility and illustrates the unique power of modelling approaches to encompass areas where experimentation would be difficult. It successfully generates and maintains a range of footfall patterns and can therefore be used to address aspects of stability, energetics and limb interference. In terms of limb interference, this was never a problem in the model. It was able to generate both lateral and diagonal sequence gaits, and the limbs did not interfere at any stage. However, when looking at quadrupedal gaits in chim-

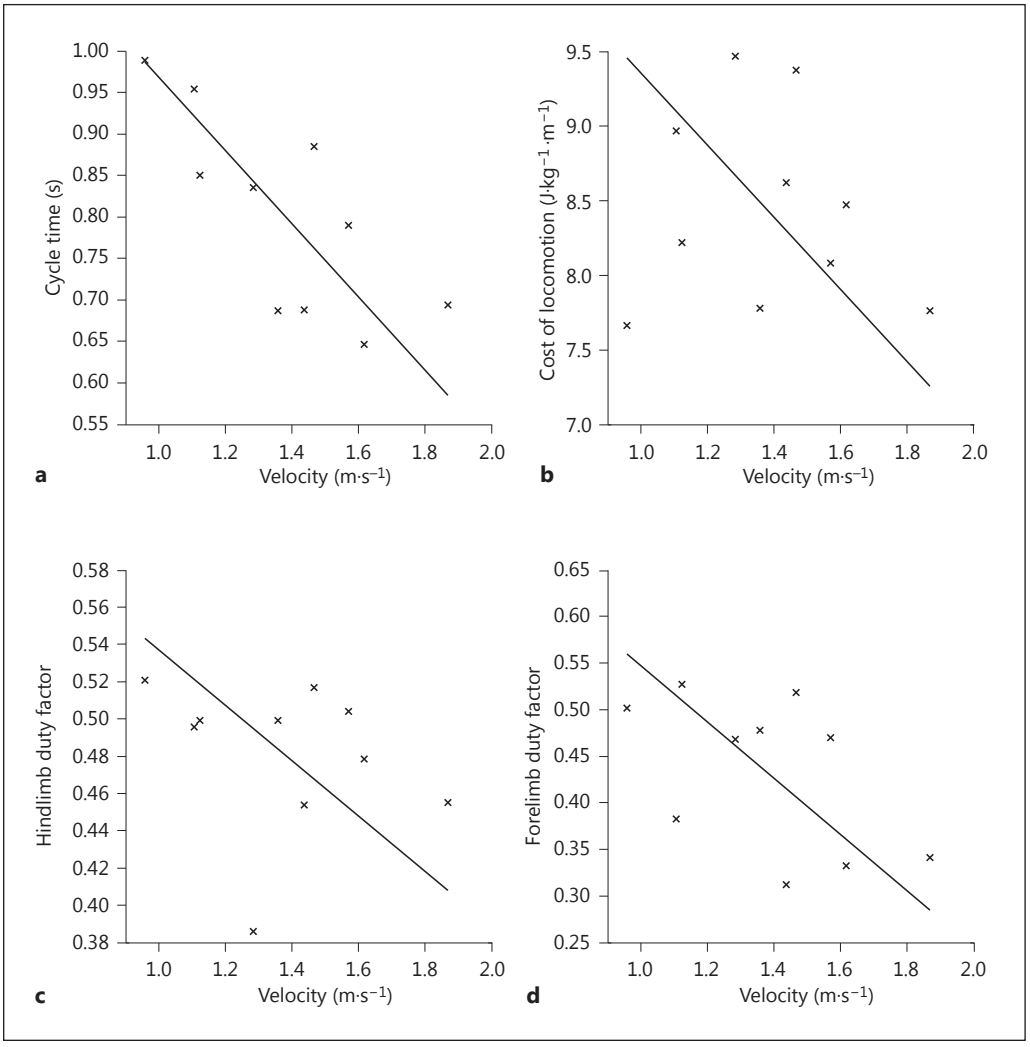

Fig. 6. Scatter plots showing the relationships between the simulation velocities and cycle time (**a**), cost of locomotion (**b**), hindlimb duty factor (**c**) and forelimb duty factor (**d**). The lines of best fit are reduced major axis regression lines. Velocity and cycle time are significantly correlated at the 5% level: Pearson linear correlation coefficient = –0.759, p = 0.011. The correlations for all the others are non-significant.

panzees we often see very close approximation of the ipsilateral fore- and hindfoot even when using diagonal gaits (fig. 8) suggesting that diagonal gaits do not show any benefit over lateral gaits in terms of reduction of limb interference in any case. Previous work also identifies overlapping of fore- and hindlimb as commonly occurring in chimpanzees as an effective solution to the limb interference problem [Hildebrand, 1965].

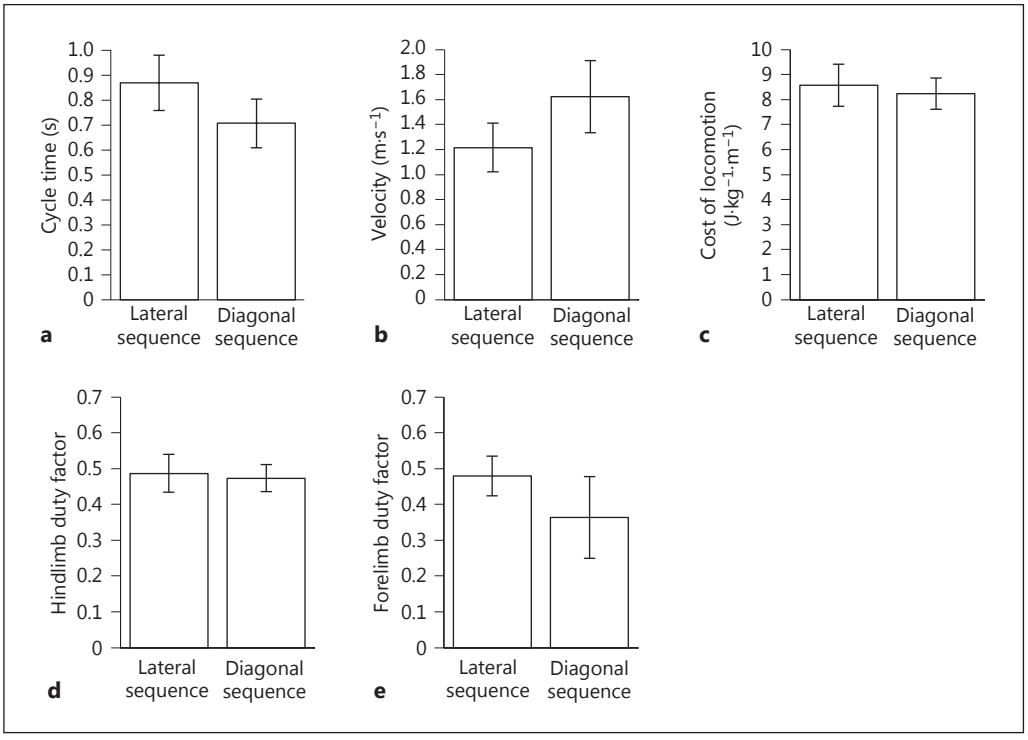

Fig. 7. Bar charts showing the effect of lateral or diagonal footfall sequences on the mean cycle time (**a**), velocity (**b**), cost of locomotion (**c**), hindlimb duty factor (**d**) and forelimb duty factor (**e**). Of these, cycle time (d.f. = 8; t = 2.737; p = 0.026), velocity (d.f. = 8; t = –3.419; p = 0.009), and forelimb duty factor (d.f. = 8; t = 2.966; p = 0.018) are statistically significant at the 5% level. The others are non-significant.

The simulation has minimising the energetic cost of locomotion as a primary goal so the different gaits generated can be compared in terms of their efficiency of energy consumption per unit distance travelled (table 6, fig. 7). The results show no significant difference in the mean value of the cost of locomotion between diagonal and lateral sequences and whilst the lowest cost of locomotion is a lateral sequence gait, it is only 0.1 $J \cdot kg^{-1} \cdot m^{-1}$ less than the next most economical, which is a diagonal sequence gait. In general it can be concluded that the simulation does not differentiate the two footfall patterns in terms of energetic cost of locomotion. However, there are some caveats with this interpretation. All the costs of locomotion generated by the model are somewhat high. The in vivo net cost of locomotion for a chimpanzee has been measured as 5.0 $J \cdot kg^{-1} \cdot m^{-1}$ for 2 running subadult chimpanzees with a mean mass of 17.5 kg [Taylor et al., 1972] and 3.8 $J \cdot kg^{-1} \cdot m^{-1}$ for 5 subadult to adult walking chimpanzees with a mean mass of 59.8 kg [Sockol et al., 2007]. The mean value obtained in the simulations was 8.438 $J \cdot kg^{-1} \cdot m^{-1}$ which is somewhat high for a 66.5-kg animal. The simulation values may reflect the fact that the system had not yet found the minimum cost of locomotion possible for the model. There are two likely reasons

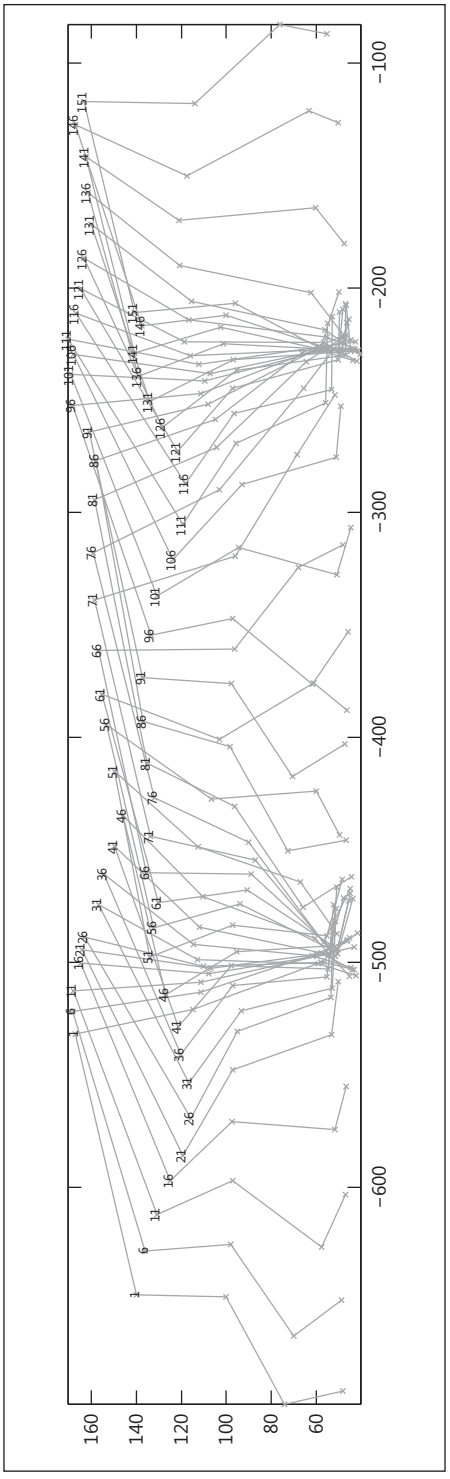

Fig. 8. Limb kinematics of a chimpanzee walking along level ground showing just the near-side limb. The distance units are arbitrary and the limb kinematics are displayed at 0.02-second intervals.

for this. The first is that insufficient computer time was available to search for a good solution given the complexity of the model. The second is that the control system for the model (10 equally timed activation levels for each of the 21 muscle action groups per gait cycle) is not sufficiently responsive to produce a really efficient gait. Unfortunately these two characteristics work against each other. If the control system is made more complex, then better solutions will exist but a good solution will be harder to find. Conversely if the control system is made simpler, then the best possible solution will be worse but it will be easier to find. In some cases there is certainly a suggestion that the solution was still improving when the optimisation algorithm was terminated to match the computational effort between runs and it would certainly be interesting to let all the runs terminate by demonstrating no further improvement. Regrettably this alternative is extremely expensive in terms of computer time. However, there is no suggestion that either of these factors would lead to a preference for lateral rather than diagonal gaits, so the interpretation that primate gait choice is constrained by energetic cost at walking speeds is unsupported.

Stability is probably the most popular explanation for primate gait choice. It is not directly an optimisation goal of the system modelled in this set of experiments: the goal state is to maximise the forward distance travelled before a limited amount of metabolic energy is used up. Clearly locomotor economy is a major factor, but the system also needs to be stable (only gaits that were stable for a distance of at least 4 m were retained for further optimisation by the gait-morphing algorithm) so stability is a hidden, but no less important, optimisation goal. If the system is unstable but efficient it will fall over before it uses all its available energy and the score will be low. Thus, the goal is actually a combination of stability and efficiency. The range of gait phases seen shows that a wide range of phase relationships can lead to stable gait, and indeed it would not be surprising if almost any phase relationship were possible, particularly at slow speeds. However, it is likely that some footfall patterns involve smaller deviations in the whole body centre of mass, or are better able to cope with larger deviations, or simply work better when they are not perfectly stable. Any of these factors would increase the likelihood of a particular solution being found and could certainly help explain why 5 of the 10 successful solutions have very similar lateral sequence/lateral couplet phase relationships. However, none of these results lends particular support to Cartmill's stability ideas [Cartmill et al., 2002]. His analysis would predict that with the short periods of fore- or hindlimb dual support seen in the simulations we would expect phase differences close to 0.5 and preferentially on the diagonal sequence side whereas the simulation results are mostly lateral and the preferred phase is between 0.15 and 0.2. In fact our data provide better support for the lateral sequence/lateral couplets ideas of Shapiro and Raichlen [2005] who suggest that lateral sequence/lateral couplets are as stable, if not more stable, than diagonal sequence/diagonal couplets although this interpretation is disputed [Cartmill et al., 2007]. Our data would also support the ideas of Vilensky and Larson [1989] who suggest that stability is not an issue and that primates are actually able to choose from a range of symmetrical gaits to distribute peak loading across various muscle groups thereby minimising fatigue and to allow specific mechanical advantages that vary with speed and substrate. The basic preference is then a matter of neural control preference and not of mechanics. It may be that, because primates tend to use both arboreal and terrestrial substrates, and arboreal substrates vary in compliance as well as surface properties, gait flexibility is the key feature of primate

locomotion rather than the choice of a specific footfall sequence [Stevens, 2006; Higurashi et al., 2009]. This is important when we consider the evolution of bipedalism. Human arm swinging occurs in a diagonal sequence although the phase relationship would equate to a trot since the forelimb is exactly out of phase with the hindlimb. Recent work [Collins et al., 2009] has shown that this arm swing can lead to a 7% decrease in metabolic energy cost; however, bipedal walking is perfectly possible without arm swinging and indeed carrying, which has been suggested as a major benefit of bipedal locomotion, requires a flexible range of upper body movements to accommodate the possible size and shape of carried loads [Watson et al., 2008]. Indeed humans demonstrate extreme gait flexibility in their brief quadrupedal phase with some 50% of infants using diagonal gaits, 20% lateral gaits with the rest using some other gait variant whilst crawling on all fours [Trettien, 1900]. In 1967, Hildebrand identified 18 different primate footfall patterns that he had observed for symmetrical gaits covering almost the full range of phase possibilities. Hildebrand's observations are primarily on free ranging animals and it is certainly the case that factors such as substrate, turning, speed change, gait change, height change will all affect gait choice under real-world conditions and these need to be considered as part of the footfall choice question.

An additional, potentially important finding of this study is that the diagonal sequences generated by the model are associated with significantly higher velocities of travel and significantly reduced forelimb duty factors, at no additional energetic cost. Both of these properties of diagonal sequence gait may be adaptively advantageous in primates, for example by helping to reduce travel time during optimal foraging, and by reducing locomotion dependence on the forelimb which (in the case of chimpanzees) has other anatomical specialisations for arboreal suspension and grasping that may interfere with its efficiency as a support member in terrestrial quadrupedalism. These findings suggest locomotion and support efficiencies that may indirectly support the energetics and skeletal loading hypotheses, respectively, but further work will be required to explore fully these properties of the computer model.

In terms of future work it would be extremely useful also to extend the model to look at non-symmetrical gait. Similar quadrupedal models have been shown to generate non-symmetrical gaits spontaneously at high speed indicating a mechanical advantage to these gait patterns [Sellers et al., 2009]. However non-symmetrical gaits are far less well-studied and need a different theoretical framework such as the new unified framework proposed by Abourachid [2003], although even this approach does not encompass the full complexity of these footfall patterns. Another area that would be worth exploring is that of gait transitions. The advantage of diagonal gaits may be that they allow efficient transition from walking to galloping without an intermediate trotting phase, which is another unusual aspect of primate locomotion. Similarly the transition from horizontal walking to vertical climbing may also benefit from a diagonal sequence, and we would propose that a multifactorial analysis will probably be necessary to understand this process fully. In general, the primate locomotor system is characterised by flexibility rather than extreme specialisation.

Conclusions

The quadrupedal chimpanzee simulation demonstrates that its morphology is compatible with a range of different gait patterns that are closely comparable in terms of their efficiency of energy ultilisation. The model shows a partial preference for lateral sequence/lateral couplet gaits suggesting that the factors favouring diagonal sequence gaits in living primates probably do not involve the energy efficiency of locomotion. It is currently unclear whether there is any stability advantage to specific gait patterns, and more work is needed in this area (for example by running the models on substrates of uneven topography, and/or variable compliance). Gait studies under real-world conditions backed up by biomechanical modelling will be necessary to understand the conditions for genuine mechanical benefit and the extent to which the observed gait choice is simply a matter of neural preference.

Acknowledgements

This work was funded by NERC and the Leverhulme Trust.

References

Abourachid A (2003). Une nouvelle méthode d'analyse des allures symétriques et asymétriques des quadrupèdes. *Comptes Rendus Biologies* 326: 625–630.
Alexander RM, Maloiy GM (1984). Stride lengths and stride frequencies of primates. *Journal of Zoology* 201: 135–152.
Bates KT, Manning PL, Hodgetts D, Sellers WI (2009). Estimating mass properties of dinosaurs using laser imaging and 3D computer modelling. *PLoS ONE* 4: e4532.
Carlson KJ (2006). Muscle architecture of the common chimpanzee *(Pan troglodytes)*: perspectives for investigating chimpanzee behavior. *Primates* 47: 218–229.
Cartmill M, Lemelin P, Schmidt D (2002). Support polygons and symmetrical gaits in mammals. *Zoological Journal of the Linnean Society* 136: 401–420.
Cartmill M, Lemelin P, Schmitt D (2007). Understanding the adaptive value of diagonal-sequence gaits in primates: a comment on Shapiro and Raichlen, 2005. *American Journal of Physical Anthropology* 133: 822–827.
Collins SH, Adamczyk PG, Kuo AD (2009). Dynamic arm swinging in human walking. *Proceedings of the Royal Society B: Biological Sciences* 276: 3679–3688.
Crompton RH, Li Y, Alexander RM, Wang W, Günther MM (1996). Segment inertial properties of primates – new techniques for laboratories and field studies of locomotion. *American Journal of Physical Anthropology* 99: 547–570.
Demes B, Larson SG, Stern JT, Jungers WL, Biknevicius AR, Schmitt D (1994). The kinetics of primate quadrupedalism – hindlimb drive reconsidered. *Journal of Human Evolution* 26: 353–374.
Griffin TM, Main RP, Farley CT (2004). Biomechanics of quadrupedal walking: how do four-legged animals achieve inverted pendulum-like movements? *Journal of Experimental Biology* 207: 3545–3558.
Higurashi Y, Hirasaki E, Kumakura H (2009). Gaits of Japanese macaques *(Macaca fuscata)* on a horizontal ladder and arboreal stability. *American Journal of Physical Anthropology* 138: 448–457.
Hildebrand M (1965). Symmetrical gaits in horses. *Science* 150: 701–708.
Hildebrand M (1967). Symmetrical gaits in primates. *American Journal of Physical Anthropology* 26: 119–130.
Hildebrand M (1968). Symmetrical gaits of dogs in relation to body build. *Journal of Morphology* 124: 353–360.
Hildebrand M (1980). The adaptive significance of tetrapod gait selection. *American Zoologist* 20: 255–267.
Hirasaki E, Kumakura H, Matano S (2000). Biomechanical analysis of vertical climbing in the spider monkey and the Japanese macaque. *American Journal of Physical Anthropology* 113: 455–472.

Kimura T (2000). Development of quadrupedal locomotion on level surfaces in Japanese macaques. *Folia Primatologica* 71: 323–333.
Kimura T, Okada M, Ishida H (1979). Kinesiological characteristics of primate walking: its significance in human walking. In *Environment, Behavior, and Morphology: Dynamic Interactions in Primates* (Morbeck ME, Preuschoft H, Gomberg N, eds.), pp 297–311. New York, Fischer.
Magna De La Croix P (1929). Los andares cuadrupedales y bipedales del hombre y del mono. *Semana Medica* 48: 1581–1588.
Méndez J, Keys A (1960). Density and composition of mammalian muscle. *Metabolism: Clinical and Experimental* 9: 184–188.
Minetti AE, Alexander RM (1997). A theory of metabolic costs for bipedal gaits. *Journal of Theoretical Biology* 186: 467–476.
Myatt JP, Crompton RH, Thorpe SKS (2011). Hindlimb muscle architecture in non-human great apes and a comparison of methods for analysing inter-species variation. *Journal of Anatomy* 219: 150–166.
Nagano A, Umberger BR, Marzke MW, Gerritsen KGM (2005). Neuromusculoskeletal computer modeling and simulation of upright, straight-legged, bipedal locomotion of *Australopithecus afarensis* (A.L. 288-1). *American Journal of Physical Anthropology* 126: 2–13.
Nakatsukasa M, Ogihara N, Hamada Y, Goto Y, Yamada M, Hirakawa T, Hirasaki E (2004). Energetic costs of bipedal and quadrupedal walking in Japanese macaques. *American Journal of Physical Anthropology* 124: 248–256.
Ogihara N, Makishima H, Aoi S, Sugimoto Y, Tsuchiya K, Nakatsukasa M (2009). Development of an anatomically based whole-body musculoskeletal model of the Japanese macaque *(Macaca fuscata). American Journal of Physical Anthropology* 139: 323–338.
Ogihara N, Makishima H, Nakatsukasa M (2010). Three-dimensional musculoskeletal kinematics during bipedal locomotion in the Japanese macaque, reconstructed based on an anatomical model-matching method. *Journal of Human Evolution* 58: 252–261.
Oishi M, Ogihara N, Endo H, Ichihara N, Asari M (2009). Dimensions of forelimb muscles in orangutans and chimpanzees. *Journal of Anatomy* 215: 373–382.
Patrick S, Noah J, Yang J (2009). Interlimb coordination in human crawling reveals similarities in development and neural control with quadrupeds. *Journal of Neurophysiology* 101: 603–613.
Payne RC, Crompton RH, Isler K, Savage R, Vereecke EE, Günther MM, Thorpe SKS, D'Août K (2006). Morphological analysis of the hindlimb in apes and humans. I. Muscle architecture. *Journal of Anatomy* 208: 709–724.
Pusey AE, Oehlert GW, Williams JM, Goodall J (2005). Influence of ecological and social factors on body mass of wild chimpanzees. *International Journal of Primatology* 26: 3–31.
Raynor AJ, Yi CJ, Abernethy B, Jong QJ (2002). Are transitions in human gait determined by mechanical, kinetic or energetic factors? *Human Movement Science* 21: 785–805.
Schmitt D (2003). Insights into the evolution of human bipedalism from experimental studies of humans and other primates. *Journal of Experimental Biology* 206: 1437–1448.
Sellers WI, Dennis LA, Crompton RH (2003). Predicting the metabolic energy costs of bipedalism using evolutionary robotics. *Journal of Experimental Biology* 206: 1127–1136.
Sellers WI, Dennis LA, Wang WJ, Crompton RH (2004). Evaluating alternative gait strategies using evolutionary robotics. *Journal of Anatomy* 204: 343–351.
Sellers WI, Manning PL, Lyson T, Stevens K, Margetts L (2009). Virtual palaeontology: gait reconstruction of extinct vertebrates using high performance computing. *Palaeontologia Electronica* 12: 11A.
Sellers WI, Pataky TC, Caravaggi P, Crompton R H (2010). Evolutionary robotic approaches in primate gait analysis. *International Journal of Primatology* 31: 321–338.
Shapiro LJ, Raichlen DA (2005). Lateral sequence walking in infant *Papio cynocephalus:* implications for the evolution of diagonal sequence walking in primates. *American Journal of Physical Anthropology* 126: 205–213.
Sockol MD, Raichlen DA, Pontzer H (2007). Chimpanzee locomotor energetics and the origin of human bipedalism. *Proceedings of the National Academy of Sciences of the United States of America* 104: 12265–12269.
Stevens NJ (2006). Stability, limb coordination and substrate type: the ecorelevance of gait sequence pattern in primates. *Journal of Experimental Zoology Part A Ecological Genetics and Physiology* 305A: 953–963.
Taylor C, Caldwell SL, Rowntree VJ (1972). Running up and down hills: some consequences of size. *Science* 178: 1096–1097.
Thorpe SKS, Crompton RH, Günther MM, Ker RF, Alexander RM (1999). Dimensions and moment arms of the hind- and forelimb muscles of common chimpanzees *(Pan troglodytes). American Journal of Physical Anthropology* 110: 179–199.
Trettien AW (1900). Creeping and walking. *American Journal of Psychology* 12: 1–57.
Videan EN, Fritz J, Murphy J (2007). Development of guidelines for assessing obesity in captive chimpanzees *(Pan troglodytes). Zoo Biology* 26: 93–104.

Vilensky J (1987). Locomotor behavior and control in human and non-human primates: comparisons with cats and dogs. *Neuroscience and Biobehavioral Reviews* 11: 263–274.
Vilensky J, Larson S (1989). Primate locomotion: utilization and control of symmetrical gaits. *Annual Review of Anthropology* 18: 17–35.
Wang W, Crompton RH, Günther MM (2003). Optimum ratio of upper to lower limb lengths in hand-carrying of a load under the assumption of frequency coordination. *Journal of Biomechanics* 36: 249–252.
Watson JC, Payne RC, Chamberlain AT, Jones RK, Sellers WI (2008). The energetic costs of load-carrying and the evolution of bipedalism. *Journal of Human Evolution* 54: 675–683.
Watson JC, Payne RC, Chamberlain AT, Jones RK, Sellers WI (2009). The kinematics of load carrying in humans and great apes: implications for the evolution of human bipedalism. *Folia Primatologia* 80: 309–328.
Winter DA (1990). *Biomechanics and Motor Control of Human Movement*. New York, Wiley & Sons.
Ziegler AC (1964). Brachiating adaptations of chimpanzee upper limb musculature. *American Journal of Physical Anthropology* 22: 15–31.